In-beam γ-ray spectroscopy of ^{248,250,252}Cf by neutron-transfer reactions using a Cf target

R. Takahashi,[1,2,*] T. Ishii,[2,3] M. Asai,[2] D. Nagae,[2] H. Makii,[2] K. Tsukada,[2] A. Toyoshima,[2] Y. Ishii,[2] M. Matsuda,[3] A. Makishima,[4] T. Shizuma,[5] T. Kohno,[6] and M. Ogawa[7]

[1]*Department of Physics, Tokyo University of Science, Noda, Chiba 278-8510, Japan*

[2]*Advanced Science Research Center, Japan Atomic Energy Agency, Tokai, Ibaraki 319-1195, Japan*

[3]*Department of Research Reactor and Tandem Accelerator, Japan Atomic Energy Agency, Tokai, Ibaraki 319-1195, Japan*

[4]*Department of Liberal Arts and Sciences, National Defense Medical College, Tokorozawa, Saitama 359-8513, Japan*

[5]*Quantum Beam Science Directorate, Japan Atomic Energy Agency, Kyoto 619-0215, Japan*

[6]*Department of Energy Sciences, Tokyo Institute of Technology, Yokohama 226-8502, Japan*

[7]*Department of Radiological Sciences, Komazawa University, Setagaya, Tokyo 154-8525, Japan*

(Received 4 February 2010; published 25 May 2010)

The ground-state bands of ^{248,250,252}Cf have been established up to the 10^+, 12^+, and 10^+ states, respectively, by in-beam γ-ray spectroscopy using neutron-transfer reactions with a 153-MeV ^{18}O beam and a highly radioactive Cf target. The deexcitation γ rays in ^{248,250,252}Cf were identified by taking coincidences with outgoing particles of $^{16-19}$O measured with Si ΔE-E detectors, and by selecting their kinetic energies. Moments of inertia of ^{248,250,252}Cf were discussed in terms of the $N = 152$ deformed shell gap.

DOI: 10.1103/PhysRevC.81.057303 PACS number(s): 23.20.Lv, 25.70.Hi, 27.90.+b

High-spin states in heavy-actinide nuclei provide us with information to predict the stability of superheavy nuclei [1]. Recently, in-beam γ-ray spectroscopy was carried out for heavy-actinide nuclei using a recoil-decay tagging technique [2] (e.g., high-spin states in ^{254}No produced by the ^{208}Pb(^{48}Ca,$2n$) reaction were studied using this technique [3–6]). By this technique, only neutron-deficient nuclei can be approached because those nuclei are produced by heavy-ion fusion reactions. Using radioactive actinide targets with a high atomic number, we can approach high-spin states in actinide nuclei near the β-stability line [7,8] and in the neutron-rich region. We have studied high-spin states in neutron-rich nuclei such as ^{240,242}U, ^{246}Pu, and ^{250}Cm by heavy-ion transfer reactions with actinide targets of $^{238}_{92}$U, $^{244}_{94}$Pu, and $^{248}_{96}$Cm [9–13]. No in-beam γ-ray experiment using a target with an atomic number higher than $_{96}$Cm, however, has been carried out because that target, such as a Cf, has high radioactivity. In the present work, we have performed an in-beam γ-ray experiment of ^{248,250,252}Cf using a Cf target.

Excited states in ^{248}Cf have been studied through the ^{249}Cf(d,t)^{248}Cf reaction [14], the β^- decay of ^{248}Bk [15], and the α decay of ^{252}Fm [16]. The ground-state band was established up to the 8^+ state; energies of the 2^+ and 4^+ states were determined precisely through the α decay of ^{252}Fm [16], and those of the 6^+ and 8^+ states were reported with an accuracy of ± 2 keV through the transfer reaction [14]. This transfer-reaction experiment also identified many two-quasiparticle states in ^{248}Cf. In ^{250}Cf, many γ transitions were observed in the EC decay of 2.22-h ^{250}Es and 8.6-h ^{250}Es, and energies of the ground-state band up to 6^+ were determined precisely [17,18]. The transfer reaction of (α, t) established the ground-state band up to 8^+, although the energy of the 8^+ state was not reported explicitly [19]. As for ^{252}Cf, the 2^+ and 4^+ states in the ground-state band and a 3^+ quasiparticle state were investigated by the EC decay of ^{252}Es [20]. In the present study, we have identified higher-spin states in the ground-state bands of ^{248,250,252}Cf up to 10^+, 12^+, and 10^+, respectively.

The experiment was carried out at the Japan Atomic Energy Agency-Tokai tandem accelerator facility [21]. We used a Cf target whose isotopic compositions were 63%, 13%, and 24% for the mass numbers of 249, 250, and 251, respectively. To reduce the total radioactivity of the target, we made a very small target with a diameter of 0.8 mm, but with an ordinary thickness of 0.45 mg/cm^2, electrodeposited onto a 0.9 mg/cm^2 aluminum foil. The total amount of this Cf target was 2.3 μg, and the total radioactivity was 1.4 MBq. The target was bombarded by a 153-MeV ^{18}O beam with 0.8 particle nA. The total dose was 1.6×10^{15} ions of ^{18}O. The beam was adjusted so as not to hit a collimator of 1.2 mm in diameter placed in front of the target.

Outgoing nuclei were detected using four sets of Si ΔE-E detectors 20 mm in diameter. γ rays emitted from residual nuclei were measured using six Ge detectors in coincidence with the outgoing nuclei. The experimental setup was the same as in Ref. [12] except that these four sets of Si ΔE-E detectors were placed at 43° with respect to the beam axis. The count rate of each Ge detector in the experiment was about 50 kcps (kilocounts per second) among which 10 kcps were associated with the decay of the Cf target itself. We recorded the particle-γ-(γ)-t coincidence data.

An E-ΔE plot obtained from the experiment is shown in Fig. 1. Outgoing nuclei were separated not only by atomic number, but also by mass number. The dashed line in Fig. 1 represents a calculated energy loss for ^{17}O particles. Figures 2(a) and 2(b) show γ-ray spectra obtained by setting the gate of the enclosed areas (a) and (b) in Fig. 1. The gate (a) in Fig. 1 is ^{17}O particles with kinetic energies corresponding to the excitation energies of ^{250}Cf between 0 and 6 MeV for the ^{249}Cf(^{18}O, ^{17}O)^{250}Cf reaction. The ^{250}Cf nucleus with these excitation energies emits no neutrons because the neutron separation energy of ^{250}Cf is 6.6 MeV. The

*takahashi.ryuta@jaea.go.jp

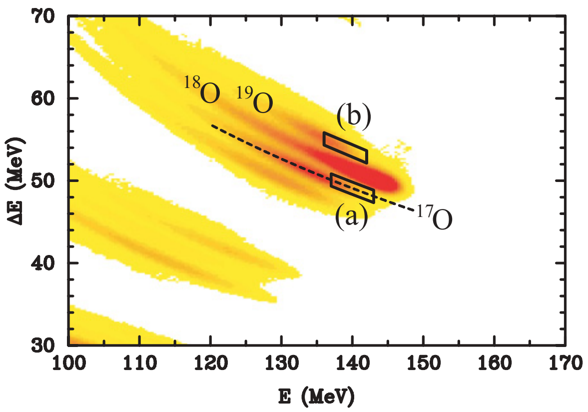

FIG. 1. (Color online) E-ΔE plot of scattered nuclei measured by a Si ΔE-E detector in the reaction of a 153-MeV ^{18}O beam with a ^{249,250,251}Cf target. The dashed line represents a calculated energy loss for ^{17}O nuclei. The enclosed areas (a) and (b) indicate the gate settings for ^{17}O + 0n and ^{19}O + 0n reaction channels, respectively.

gate (b) is ^{19}O particles with kinetic energies corresponding to the excitation energies of ^{248}Cf between 0 and 6 MeV for the ^{249}Cf(^{18}O,^{19}O)^{248}Cf reaction.

We observed 99.2-, 154.3-, 207.7-, and 258.9-keV γ rays having almost equal energy spacings, as shown in Fig. 2(a). These four γ rays were coincident with each other. The 307.4-keV γ ray was also found to be coincident with these γ rays. Because the 99.2- and 154.3-keV transitions observed

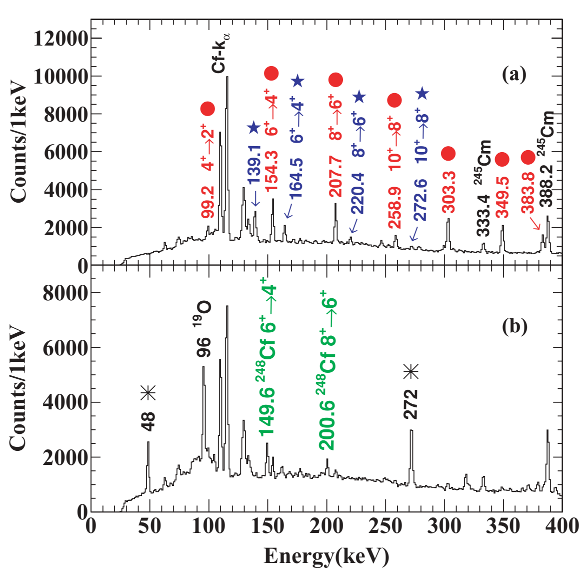

FIG. 2. (Color online) (a) γ-ray spectrum obtained by setting the gate on ^{17}O + 0n [gate (a) in Fig. 1]. The kinetic energies of ^{17}O correspond to the excitation energies of ^{250,252}Cf between 0 and 6 MeV for the ^{249,251}Cf(^{18}O,^{17}O)^{250,252}Cf reaction. The γ rays marked with circles and stars are transitions in ^{250}Cf and ^{252}Cf, respectively. The 303.3-, 349.5-, and 383.8-keV γ rays are transitions deexciting the 4^- state with the configuration of $\{\nu[734]9/2^-;\nu[620]1/2^+\}$ in ^{250}Cf [18]. The 139.1-keV γ ray is the transition deexciting the 3^+ state with the configuration of $\{\nu[620]1/2^+;\nu[613]7/2^+\}$ in ^{252}Cf [20]. (b) γ-ray spectrum obtained by setting the gate on ^{19}O + 0n [gate (b) in Fig. 1]. The γ rays with asterisks have not been assigned yet.

TABLE I. Observation of γ rays in the ground-state bands of ^{248,250,252}Cf for different gates of $^{16-19}$O. Gates where γ rays in the ground-state bands of ^{248,250,252}Cf were observed are marked with a cross. Gates used for analysis of γ-ray properties are marked with an asterisk. Gates of $^{16-19}$O + 0n and $^{16-19}$O + 1n correspond to the excitation energies of 0–6 MeV and 6–12 MeV in Cf, respectively. Reaction channels for producing ^{248,250,252}Cf are listed in the bottom row. Crosses within parentheses indicate that the observation of these γ rays would come from an admixture of neighboring reaction channels.

Gate	^{248}Cf	^{250}Cf	^{252}Cf
^{16}O + 0n		(×)	×
^{16}O + 1n		×	×
^{17}O + 0n		*	*
^{17}O + 1n		×	(×)
^{18}O + 0n		×	
^{18}O + 1n	×	×	
^{19}O + 0n	*	×	
^{19}O + 1n	×	(×)	
	^{249}Cf(^{18}O, ^{18}On) ^{249}Cf(^{18}O, ^{19}O) ^{250}Cf(^{18}O, ^{19}On)	^{249}Cf(^{18}O, ^{16}On) ^{249}Cf(^{18}O, ^{17}O) ^{250}Cf(^{18}O, ^{17}On) ^{250}Cf(^{18}O, ^{18}O) ^{251}Cf(^{18}O, ^{18}On) ^{251}Cf(^{18}O, ^{19}O)	^{250}Cf(^{18}O, ^{16}O) ^{251}Cf(^{18}O, ^{16}On) ^{251}Cf(^{18}O, ^{17}O)

in the present work have the same energy as the $4^+ \rightarrow 2^+$ [99.16(1) keV] and $6^+ \rightarrow 4^+$ [154.35(6) keV] transitions in the ground-state band of ^{250}Cf [18], we have identified the γ rays of 207.7, 258.9, and 307.4 keV as well as the γ rays of 99.2 and 154.3 keV as the transitions in the ground-state band of ^{250}Cf.

γ transitions in the ground-state band of ^{250}Cf were also observed in other reaction channels. For example, these γ rays were observed in the ^{16}O gate with kinetic energies corresponding to the excitation energies between 6 and 12 MeV in ^{251}Cf, which is high enough to evaporate one neutron from ^{251}Cf. These γ rays should be produced by the reaction channel of ^{249}Cf(^{18}O, ^{16}On)^{250}Cf; the gate setting of this reaction channel is denoted by ^{16}O + 1n. Furthermore, the γ rays in ^{250}Cf were observed in coincidence with ^{19}O + 0n, produced in the reaction channel of ^{251}Cf(^{18}O, ^{19}O)^{250}Cf. Because the target comprises three isotopes, we took account of several reaction channels producing ^{250}Cf. In Table I, we summarize the gates in which γ rays in the ground-state bands of ^{248,250,252}Cf were observed. The reaction channels for producing ^{248,250,252}Cf are listed in the bottom row. The ambiguity of the excitation energy is approximately 2 MeV owing to the covering angles of the Si ΔE-E detectors. Therefore, the gate represented by ^{16}O + 1n, for example, includes components of reaction channels of (^{18}O, ^{16}O + 0n) and (^{18}O, ^{16}O + 2n).

We have identified 164.5-, 220.4-, and 272.6-keV γ rays observed in Fig. 2(a) as the ground-state band transitions in ^{252}Cf. These γ rays have almost equal energy spacings, and are coincident with each other. Figure 3 shows a sum of γ-γ coincidence spectra gated on 164.5-, 220.4-, and

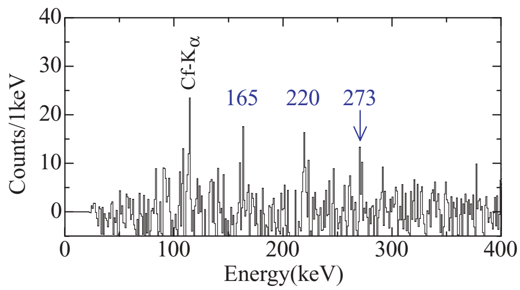

FIG. 3. (Color online) γ-γ coincidence spectrum for ground-state band transitions in ^{252}Cf, obtained by the sum of spectra in coincidence with 164.5-, 220.4-, and 272.6-keV γ rays.

272.6-keV γ-ray peaks. These γ rays are considered to be populated by the ^{251}Cf(^{18}O, ^{17}O)^{252}Cf reaction. The intensity ratio of this 164.5-keV γ peak to the 154.3-keV γ peak of ^{250}Cf is approximately one-third, consistent with the composition ratio of ^{249}Cf to ^{251}Cf in the target. The 164.5- and 220.4-keV γ rays were observed as well in the $^{16}O + 0n$ and $^{16}O + 1n$ gates, which correspond to the reaction channels of ^{250}Cf(^{18}O, ^{16}O)^{252}Cf and ^{251}Cf(^{18}O, ^{16}On)^{252}Cf, respectively. This fact confirms the assignment of these γ rays to ^{252}Cf. The observation of γ rays in ^{252}Cf in the gate of $^{17}O + 1n$ would come from the admixture of the (^{18}O, ^{17}O) reaction channel.

We have assigned 149.6- and 200.6-keV γ transitions observed in Fig. 2(b) as the ground-state band transitions in ^{248}Cf. These γ rays are coincident with the 249.3-keV γ ray. These three γ rays have almost equal energy spacings. They are considered to be populated by the ^{249}Cf(^{18}O, ^{19}O)^{248}Cf reaction. The 149.6- and 200.6-keV γ rays were only observed in the gates of $^{18}O + 1n$, $^{19}O + 0n$, and $^{19}O + 1n$. This fact confirms the assignment of these γ rays to ^{248}Cf.

Level schemes of the ground-state bands of ^{248,250,252}Cf are shown in Fig. 4. We have extended high-spin states of the ground-state bands of ^{248,250,252}Cf up to 10^+, 12^+, and 10^+, respectively. Energies, relative intensities, and in-plane to out-of-plane anisotropies, $I_\gamma(\text{in})/I_\gamma(\text{out})$, for the γ transitions in the ground-state bands of ^{248,250,252}Cf are summarized in Table II. The relative intensities of the γ rays in Table II are normalized to the intensity of the $4^+ \rightarrow 2^+$ transition in ^{250}Cf. The $I_\gamma(\text{in})/I_\gamma(\text{out})$ values for the transitions in ^{250}Cf are larger than unity, which confirms that these transitions are stretched quadrupole transitions [23,24].

The moments of inertia for the ground-state band of ^{252}Cf are plotted as a function of squared rotational frequency in Fig. 5. $I^{(1)}$ and $I^{(2)}$ represent the kinematic and dynamic moments of inertia, and ω is the rotational frequency [9]. The $I^{(1)}$ values were derived from the spins as well as the γ-ray energies. The solid line in Fig. 5 is the fit of $I^{(1)}$ to $J_0 + \omega^2 J_1$, where J_0 and J_1 are constants. The $I^{(2)}$ values calculated by $J_0 + 3\omega^2 J_1$ are drawn as the dashed line in Fig. 5. The J_0 values of ^{248,250,252}Cf ($N = 150, 152, 154$) were obtained as 72.10(5), 70.15(1), and 65.43(5)$\hbar^2$ MeV^{-1}, respectively. Sobiczewski *et al.* [25] predicted that a moment of inertia has a larger value at $N = 152$ than those of neighboring nuclei because the pairing correlation is weak at $N = 152$ owing to the deformed shell gap. According to their calculation, moments of inertia of $_{100}$Fm and $_{102}$No have a clear peak at $N = 152$, but those of $_{94}$Pu do not. This is caused because the deformed shell gap at $N = 152$ becomes narrower for nuclei

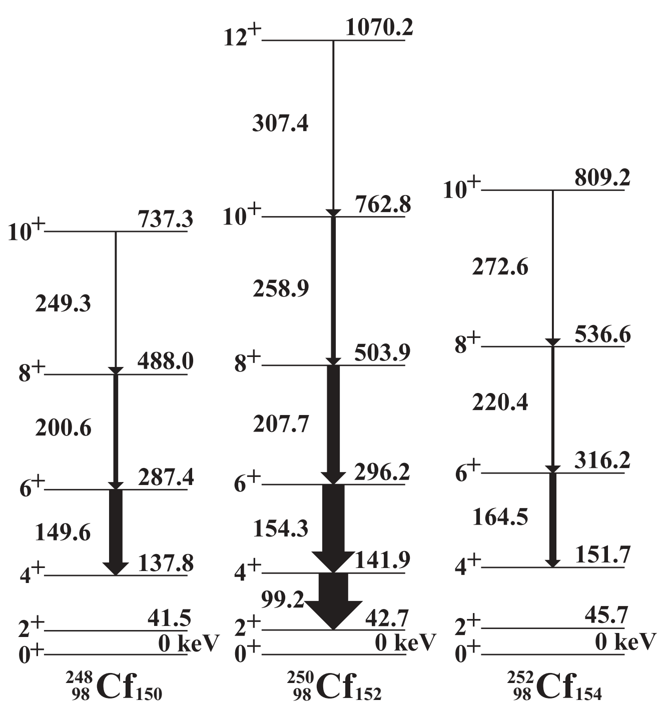

FIG. 4. Level schemes of ^{248,250,252}Cf. The γ-ray and level energies are in units of kiloelectron volts. Energies of the 2^+ and 4^+ states in ^{248}Cf, those of the states up to 6^+ in ^{250}Cf, and those of the 2^+ and 4^+ states in ^{252}Cf were taken from Refs. [16,18,20].

TABLE II. Energies and relative intensities of γ rays in ^{248,250,252}Cf. Total internal conversion coefficients α_T for $E2$ transitions were taken from Ref. [22]. In-plane to out-of-plane intensity ratios, $I_\gamma(\text{in})/I_\gamma(\text{out})$, are also given.

		^{248}Cf		
$I_i \rightarrow I_f$	E_γ (keV)	I_γ	$I_\gamma(1+\alpha_T)$	$I_\gamma(\text{in})/I_\gamma(\text{out})$
$6^+ \rightarrow 4^+$	149.6(1)	9.4(5)	44(2)	1.10(12)
$8^+ \rightarrow 6^+$	200.6(1)	6.8(6)	14(1)	1.05(18)
$10^+ \rightarrow 8^+$	249.3(5)[a]	2.4(13)[a]	4(2)[a]	
		^{250}Cf		
$I_i \rightarrow I_f$	E_γ (keV)	I_γ	$I_\gamma(1+\alpha_T)$	$I_\gamma(\text{in})/I_\gamma(\text{out})$
$4^+ \rightarrow 2^+$	99.2(1)	4.2(4)	100(10)	1.01(23)
$6^+ \rightarrow 4^+$	154.3(1)	17.6(6)	75(3)	1.17(7)
$8^+ \rightarrow 6^+$	207.7(1)	21.2(9)	42(2)	1.34(9)
$10^+ \rightarrow 8^+$	258.9(2)	9.7(6)	14(1)	1.38(19)
$12^+ \rightarrow 10^+$	307.4(5)[a]	2.9(12)[a]	4(2)[a]	
		^{252}Cf		
$I_i \rightarrow I_f$	E_γ (keV)	I_γ	$I_\gamma(1+\alpha_T)$	$I_\gamma(\text{in})/I_\gamma(\text{out})$
$6^+ \rightarrow 4^+$	164.5(1)	6.3(5)	22(2)	1.33(22)
$8^+ \rightarrow 6^+$	220.4(3)	4.7(5)	8(1)	1.14(33)
$10^+ \rightarrow 8^+$	272.6(5)	2.8(5)	4(1)	1.35(44)

[a]Obtained from γ-γ coincidence data.

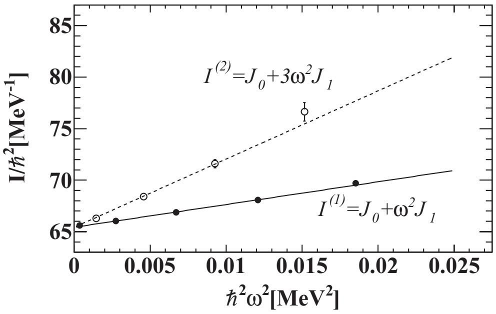

FIG. 5. Plot of moments of inertia for the ground-state band of ^{252}Cf versus squared rotational frequency ω^2. The closed and open circles represent the kinematic moments of inertia $I^{(1)}$ and the dynamic moments of inertia $I^{(2)}$, respectively. The solid line is the fit of $I^{(1)}$ to $J_0 + \omega^2 J_1$. The dashed line is calculated by $J_0 + 3\omega^2 J_1$, using J_0 and J_1 obtained from the fit of $I^{(1)}$.

with lower atomic numbers [11]. Their calculation shows that the moments of inertia of $_{98}$Cf still have a peak at $N = 152$. On the other hand, the experimental J_0 value of ^{248}Cf$_{150}$ is larger than that of ^{250}Cf$_{152}$. More sophisticated calculations are required to reproduce the experimental results.

We have found that the moments of inertia of the ground-state bands in ^{248,250,252}Cf gradually increase up to the 10^+, 12^+, and 10^+ states, respectively. At higher-spin states, effects of rotation alignment originating from high-j orbitals, such as $\pi i_{13/2}$, $\nu j_{15/2}$, and $\nu k_{17/2}$, should appear. Sun [26] predicted that a band crossing occurs around $I = 24$. By measuring higher-spin states, we could obtain information regarding single-particle energies of high-j orbitals. These energies provide us with information relating to the stability of superheavy nuclei.

In conclusion, in-beam γ-ray spectroscopy of Cf isotopes has been performed for the first time using neutron-transfer reactions and a highly radioactive Cf target. The ground-state bands of ^{248,250,252}Cf were extended up to the 10^+, 12^+, and 10^+ states, respectively. The γ rays in each nucleus were identified by taking coincidence with outgoing particles and by selecting their kinetic energies using Si ΔE-E detectors. The present experiment demonstrated that a target with high radioactivity or on the order of micrograms can be used in in-beam γ-ray spectroscopy. The moments of inertia of ^{248,250,252}Cf$_{150,152,154}$ does not clearly show the effect of the $N = 152$ deformed shell gap.

[1] A. V. Afanasjev, T. L. Khoo, S. Frauendorf, G. A. Lalazissis, and I. Ahmad, Phys. Rev. C **67**, 024309 (2003).
[2] R.-D. Herzberg and P. T. Greenlees, Prog. Part. Nucl. Phys. **61**, 674 (2008).
[3] P. Reiter *et al.*, Phys. Rev. Lett. **82**, 509 (1999).
[4] M. Leino *et al.*, Eur. Phys. J. A **6**, 63 (1999).
[5] P. Reiter *et al.*, Phys. Rev. Lett. **84**, 3542 (2000).
[6] S. Eeckhaudt *et al.*, Eur. Phys. J. A **26**, 227 (2005).
[7] G. Hackman *et al.*, Phys. Rev. C **57**, R1056 (1998).
[8] W. Spreng *et al.*, Phys. Rev. Lett. **51**, 1522 (1983).
[9] T. Ishii, S. Shigematsu, M. Asai, A. Makishima, M. Matsuda, J. Kaneko, I. Hossain, S. Ichikawa, T. Kohno, and M. Ogawa, Phys. Rev. C **72**, 021301(R) (2005).
[10] T. Ishii *et al.*, Phys. Rev. C **76**, 011303(R) (2007).
[11] H. Makii *et al.*, Phys. Rev. C **76**, 061301(R) (2007).
[12] T. Ishii *et al.*, Phys. Rev. C **78**, 054309 (2008).
[13] T. Ishii *et al.*, J. Phys. Soc. Jpn. **75**, 043201 (2006).
[14] K. Katori, I. Ahmad, and A. M. Friedman, Phys. Rev. C **78**, 014301 (2008).
[15] H. C. Griffin, I. Ahmad, A. M. Friedman, and L. E. Glendenin, Nucl. Phys. A **303**, 265 (1978).
[16] I. Ahmad and J. L. Lerner, Nucl. Phys. A **413**, 423 (1984).
[17] I. Ahmad and R. K. Sjoblom, Phys. Rev. C **22**, 1226 (1980).
[18] M. S. Freedman, I. Ahmad, F. T. Porter, R. K. Sjoblom, R. F. Barnes, J. Lerner, and P. R. Fields, Phys. Rev. C **15**, 760 (1977).
[19] S. W. Yates, I. Ahmad, A. M. Friedman, K. Katori, C. Castaneda, and T. E. Ward, Phys. Rev. Lett. **36**, 1125 (1976).
[20] P. R. Fields, I. Ahmad, R. F. Barnes, R. K. Sjoblom, and W. C. McHarris, Nucl. Phys. A **208**, 269 (1973).
[21] T. Ishii *et al.*, in *JAEA-Tokai Tandem Annual Report 2008*, JAEA-Review 2009-036, pp. 3–4.
[22] T. Kibédi, T. W. Burrows, M. B. Trzhaskovskaya, P. M. Davidson, and C. W. Nestor Jr., Nucl. Instrum. Methods A **589**, 202 (2008); Conversion Coefficients Calculator BrIcc v2.2b [http://wwwrsphysse.anu.edu.au/nuclear/bricc/].
[23] T. Ishii, M. Asai, A. Makishima, I. Hossain, M. Ogawa, J. Hasegawa, M. Matsuda, and S. Ichikawa, Phys. Rev. Lett. **84**, 39 (2000).
[24] M. Asai, T. Ishii, A. Makishima, I. Hossain, M. Ogawa, and S. Ichikawa, Phys. Rev. C **62**, 054313 (2000).
[25] A. Sobiczewski, I. Muntian, and Z. Patyk, Phys. Rev. C **63**, 034306 (2001).
[26] Y. Sun, Nucl. Phys. A **834**, 41c (2010).